

- and A. J. Rubin, Eds. (Ann Arbor Science, Ann Arbor, MI, 1981), pp. 183–217.
30. R. O. James, in *ibid.*, pp. 219–261.
 31. P. W. Schindler and W. Stumm, in *Aquatic Surface Chemistry*, W. Stumm, Ed. (Wiley, New York, 1987), pp. 83–110.
 32. D. A. Dzombak and F. M. M. Morel, *Surface Complexation Modelling* (Wiley, New York, 1990).
 33. P. R. Unwin and A. J. Bard, in preparation.
 34. A. Blum and A. Lasaga, *Nature* **331**, 431 (1988).
 35. P. R. Unwin and A. J. Bard, in preparation.
 36. W. J. Albery and M. L. Hitchman, *Ring-Disc Electrodes* (Clarendon, Oxford, 1971).
 37. A. T. Hubbard and F. C. Anson, in *Electroanalytical Chemistry*, A. J. Bard, Ed. (Dekker, New York, 1970), vol. 4, p. 129.
 38. F. Zhou, P. R. Unwin, A. J. Bard, unpublished results.
 39. J. Kwak, C. Lee, F. Anson, personal communication.
 40. E. R. Scott, H. S. White, J. B. Phipps, *J. Membr. Sci.* **58**, 71 (1991).
 41. O. E. Hüsler, D. H. Craston, A. J. Bard, *J. Vac. Sci. Technol. B* **6**, 1873 (1988).
 42. Y.-M. Wu, F.-R. F. Fan, A. J. Bard, *J. Electrochem. Soc.* **136**, 885 (1989).
 43. D. Mandler and A. J. Bard, *ibid.*, p. 3143.
 44. ———, *ibid.* **137**, 1079 (1990).
 45. ———, *ibid.*, p. 2468.
 46. The support of this research by grants from the Robert A. Welch Foundation, the Texas Advanced Research Program, and the NSF is gratefully acknowledged. P.R.U. thanks SERC for the award of a NATO fellowship. We thank D. M. Zeigler for providing the mitochondria used in this work.

Chemical Microsensors

R. C. HUGHES, A. J. RICCO, M. A. BUTLER, S. J. MARTIN

Recent developments in the field of chemical microsensors are leading to new applications for which these devices have the potential to supplement or replace traditional analytical chemical instrumentation. The fundamentals of current microelectronic, acoustic wave, optical fiber, and electrochemical microsensors are presented,

and a few recent, exciting results in these areas are described. Although future opportunities in the microsensor field are numerous, many significant problems, the majority of them related to the materials utilized for the chemically sensitive layers that are the “front end” of these devices, remain to be explored and solved.

MANY TASKS FACED BY MODERN ANALYTICAL CHEMISTRY are difficult to solve with conventional, laboratory-based analytical instruments for reasons of size, speed, or cost. The chemical microsensor finds its niche when a continuous measurement of a chemical concentration is required from a number of locations, and only a small space or low power (or both) are available for each sensor. As a result of interest in such potential applications, many researchers are active in this field, and a great deal of literature exists (1–4).

Some of the applications that have been cited by existing or potential users of microsensors who believe that existing instrumentation is inadequate are listed in Table 1. Many such applications arise because time does not permit obtaining a sample and returning it from the field to the laboratory. Furthermore, in many cases it is unnecessary to have a detailed chemical analysis of each sample: only the concentration is of interest because the chemical species is already known for a particular site. In such cases, an inexpensive, nonselective microsensor may be the ideal solution.

As a result of the roots of microsensors in microelectronic mass production technology, the incremental cost of microsensors can be quite low. In contrast, the cost of chemical monitoring with conventional laboratory apparatus can be relatively high. An example is the analysis of a single sample from a well for monitoring ground-water contamination: the cost can exceed \$300 by the time the sample is collected, transported to an analytical laboratory, and analyzed. In addition, such an analysis only gives one concentration data point in time and space, with the chance that the removal and transportation of the sample may have altered its chemical composition.

In addition to the advantages of real-time, in situ, low-cost monitoring, chemical microsensors can, in some instances, provide very high sensitivity. The “micro” in microsensor becomes very important if the limits of sensitivity depend on the absolute number of molecules to be detected. An example is when a fixed, small volume sample (for example, the contents of a living cell) is all that is available, and essentially all of the desired species can be delivered to the microsensor. The response of chemical microsensors usually depends on the number of interacting molecules per unit area; thus, the smaller the device, the fewer molecules can be detected. In some instances, however, the limiting sensitivity may be related to the concentration of the species to be detected, in which case the size of the device has little effect on sensitivity. An example of this is monitoring a low concentration but essentially unlimited volume sample, such as an underground aquifer or a region of the atmosphere. Knowledge of the nature and extent of the sample is thus important in determining whether a microsensor can provide a sensitivity advantage. These concepts may falter for ultrasmall (submicrometer) sensor structures, in which the size of the sensing structure becomes comparable to the size or diffusion lengths (or both) of the molecules being detected.

The interface between the physical transducer and the chemical transducer can be complex. Thus, predicting the performance of a sensor often requires detailed knowledge not only of the device physics and the chemistry of the sensing layer, but of the interplay between the two as well. Although the principles of operation of the micro- and optoelectronic devices that serve as platforms for chemical microsensors are often well known to physicists and electrical engineers, chemical transducer coatings are alien to the world of microelectronics. Indeed, billions of dollars have been spent to stabilize microelectronic devices against the changes caused by chemical reactions. For example, electrically mobile sodium and

The authors are with the Microsensor Division, Sandia National Laboratories, Albuquerque, NM 87185.

Table 1. Present and potential applications for chemical microsensors.

Application	Examples
Environmental monitoring of toxic chemicals	Trichloroethylene in air, soil, and ground water
Determining status of expensive equipment	Transformers, turbines, airplanes
Internal combustion engine exhaust analysis	O ₂ , NO _x , CO, hydrocarbons
Explosive gas monitoring	Hydrogen leaks in spacecraft, natural gas leaks
Locating illegal drugs, illegal explosives, and illegal drug manufacturing	Portals in airports, portable monitoring
Inexpensive sensors for home hazards	Carbon monoxide, natural gas
Critical monitoring of chemical processes	Material separation, manufacturing and waste stream control
In vivo sensing of critical chemical concentrations	Ions, pH, pO ₂ , pCO ₂ , glucose, and so forth
Research on complex chemical reactions	Reactive flows

potassium ions are an unwanted contaminant in the vital, thermally grown SiO₂ layer on the single crystal Si that is the heart of the integrated circuit (5).

This article focuses on recent developments in the field of chemical microsensors that attempt to marry physical transducers based on microelectronic and optoelectronic technologies with the thin films and coatings that serve as chemical transducers. The chemical transducer is typically a thin film that quickly and, in ideal cases, reversibly alters a physical property in the presence of the molecules to be detected. In Table 2, some of the chemical interactions that have been employed for microsensors are listed along with the various physical perturbations caused by those interactions. There is no particular correlation between any one of the chemical interactions and any one physical perturbation. Listed as well are some of the physical transducers that detect these perturbations. This article is organized around different classes of physical transducers, which is simpler than grouping the ways in which chemical and physical transducers interface: a given chemical interaction often can be detected by several entirely different physical transducers.

Table 2. Typical chemical interactions, physical perturbations, and physical transducers utilized for chemical microsensors. Entries in the "Chemical interaction" column are not correlated with those in the other two columns; that is, any chemical interaction typically results in several physical perturbations from various categories. The center and right-hand

Chemical interaction	Physical perturbation	Physical transducer
Adsorption: chemisorption and physisorption on external surfaces Absorption: dissolution into polymers or gels and adsorption on internal surfaces of rigid porous materials	Electronic: dipole moment, dielectric coefficient, conductivity, work function, surface charge Optical: reflectivity, absorptivity, emissivity, transmission, fluorescence, spectral distribution, refractive index, optical path length	Electronic device: ChemFET, ISFET, diode, capacitor, Kelvin probe, chemiresistor Optical device: optical fiber (micromirror, evanescent detection, interferometer, bifurcated pair or bundle), wave guide, microspectrophotometer
Irreversible compound formation	Mechanical: density (mass or volume change or both), pressure, strain, modulus, viscosity, viscoelasticity	Acoustic wave device: surface acoustic wave, acoustic plate mode, Lamb wave, flexural plate wave, quartz crystal microbalance
Catalytic dissociation; a precursor to absorption or adsorption	Electrochemical: redox potential (pH), electroactivity, electroactive concentration	Electrochemical device: ChemFET, ISFET, coated wire, microelectrode, interdigital (micro)electrode array, amperometric electrode
Selective binding: antibody-antigen, chemical complexation	Thermal: temperature, heat capacity	Thermal device: pyroelectric detector, thermocouple, resistance-temperature device

Microelectronic Silicon Chemical Sensors—The Chemical Amplifier

Silicon microelectronics are often touted as giving the most sensitive and stable measurements of physical phenomena. In the realm of chemical detection, biological systems unequivocally outperform all of the microelectronically based chemical sensors in terms of sensitivity and selectivity, despite rapid progress in recent years. One of the best studied examples of biological chemical detection is the sex attractant receptor of moths. Single molecule detection of the sex attractant molecule (bombykol) can be claimed if the firing of a single neuron is monitored with a probe. However, if a response by the moth is the criterion, it has been shown that an airstream containing 1000 molecules per cubic centimeter is required (6); this is 1 part in 10¹⁶ at standard temperature and pressure (STP). The microsensor of the moth is a receptor on a membrane protein that is part of the ion channel in the nerve cell wall.

The mechanisms of operation of these ion channels are under intense discussion (7, 8); basically, they operate as chemical amplifiers: one molecule of analyte binds specifically to the receptor protein, and the conductance of the channel then increases dramatically. This sort of mechanical-to-electrical amplifier has been demonstrated on single ion channels in the laboratory in artificial membranes (9), but real world, rugged chemical microsensors based on these proteins pose many developmental problems.

In contrast, the chemical amplifier based on the electric field effect in Si, although similar in response, operates on different principles. The simplest example is a sensor for H₂ based on a Si field-effect transistor invented by Lundström and colleagues in the mid-1970s (10). The presence of H₂ causes a marked increase in the current through the conducting channel of the field-effect transistor. It is not a mechanical, conformational effect but an electrostatic effect that is used.

The simplest form of the field effect device is shown in Fig. 1. It is a metal/insulator/semiconductor capacitor. The metal is a thin film of Pd and the semiconductor is usually lightly doped Si. At equilibrium, the Fermi levels of the metal and semiconductor must be the same, but no charge can flow through the SiO₂ insulator. Charge can collect on the various surfaces and interfaces, and in the band diagram shown in Fig. 1 a net negative charge has collected on the Pd and a net positive charge on the Si (in the form of the fixed, positively charged donor atoms). The capacitance of this layered

columns are arranged so that perturbations match up with the most commonly used transducers for those effects, but "crossovers" are typical: acoustic wave devices can detect electronic and thermal perturbations in addition to mechanical effects. ChemFET = chemically sensitive field-effect transistor.

structure is easily measured with an alternating current (AC) method, and its magnitude depends on the static (DC) bias (which is zero in the band diagram). The capacitance varies with DC bias in this case because it is the result of two capacitances in series, namely, the capacitance of the SiO_2 layer and that of the surface layer of the Si (also known as the depletion layer); the capacitance of the semiconductor layer is proportional to the charge required to balance the charge on the Pd metal (5). The so-called flat-band condition occurs when the DC bias cancels the charge on the Pd and the thickness of the depletion region in the Si approaches zero, causing the conduction and valence bands in Fig. 1 to flatten.

In the flat-band condition, the device becomes a very sensitive detector for any additional charge that appears in the insulator anywhere between the Pd and Si/ SiO_2 interface. This distance can be as little as 75 Å without violating the simple case of no charge flowing through the insulator. Typically, the thickness is 200 to 2000 Å for durability.

This structure can be used to detect H_2 at room temperature because H_2 molecules readily dissociate on the surface of the Pd, and H atoms then diffuse very rapidly through the metal. Fortuitously, the Pd/ SiO_2 interface has traps for H that, when occupied, have dipole moments oriented with the positive end toward the Si layer (Fig. 1). We made a crude measurement of the dipole moment and the areal density of traps by titrating the traps with a beam of H^+ ions (11), the result of which was a density of 10^{15} traps per square centimeter with a 0.3-D dipole moment when filled. Because of the solubility and mobility of H in Pd, equilibrium is established between the gas phase and the interfacial traps; the fraction of sites occupied thus depends on the partial pressure of H_2 in the gas phase (10). Because of the great immunity of these microelectronic devices to other influences, a change in 1×10^{11} traps per square centimeter can be easily observed, which means that in a small device of area 10^{-3} cm^2 , 10^8 H atoms can be measured. The equilibrium between the traps and the gas phase H_2 at room temperature is strongly in favor of the traps (by $\sim 1 \text{ eV}$) so that in a proof-of-principle experiment with atomically clean Pd, a step in H_2 pressure from 6×10^{-10} to 1×10^{-9} torr was observed in a few seconds (12). Though impressive, this detection limit is still four orders of magnitude less sensitive than the moth receptor structure at room temperature. A

Fig. 1. A field-effect chemical sensor for H_2 , shown in the top schematic as a Pd insulator-semiconductor capacitor. Orientations of the dipole moments of H atoms trapped at the interface are shown as well as a simple circuit for measuring the series capacitance of the insulator-semiconductor layered structure. The bottom diagram shows the effect of the charges and work functions of the materials on electric potentials (and fields) in the layers. Here ϕ_M is the work function of Pd metal; ϕ_B is the barrier height for electrons, related to χ , the electron affinity of the Si; E_G is the Si band gap; and E_C , E_F , and E_V are the energies of the conduction band, the Fermi level for electrons, and the valence band, respectively. The depletion layer in the Si contains fixed, positively charged donor atoms that "bend" the bands. Some extra positive charge is shown in the SiO_2 layer; it could be due to the dipoles shown above.

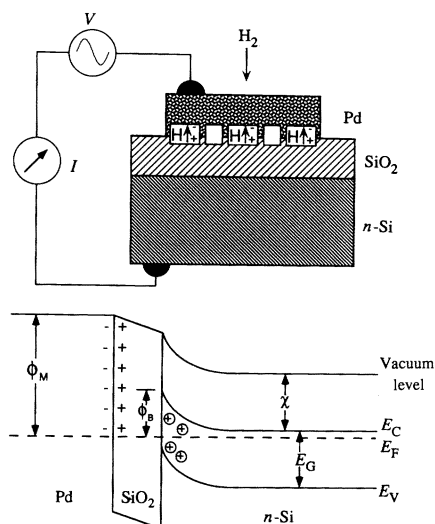
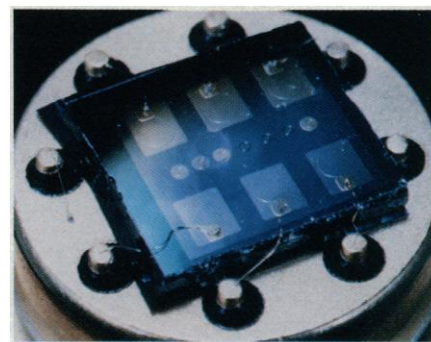


Fig. 2. An array of six independent chemically sensitive field-effect devices on a silicon chip. The chip measures about 2 mm by 3 mm and is mounted in a standard TO-5 header. The circles down the center are alignment markers for the masks that allow a different metallization to be deposited on each of the six sensor sites.



concentration of 10^3 H_2 molecules per cubic centimeter would, in principle, be detectable, but there are two practical problems: the background pressure of H_2 in a stainless steel ultrahigh vacuum chamber is far in excess of such levels, and the time for enough H_2 to impact the surface of the device to provide a measurable response would be several hours. The advantage of the moth is in large part a result of its ability to detect a relatively small number of a unique, biomanufactured molecule that has no natural interferants (H_2 is omnipresent at low concentrations).

Although Pd-gated devices are somewhat selective for the H_2 molecule at room temperature, they do respond to a number of other molecules, including ethanol, ethylene, acetylene, ammonia, and formic acid, that can dissociate on the Pd surface to yield atomic H (13, 14). Oxidizing gases can also be detected if a known amount of H_2 is mixed with the analyte gas stream. To facilitate the analysis of gas mixtures, one can use arrays of sensors, each with a different modification of the Pd gate. One such array is shown in Fig. 2, in which six catalytic gate sites are fabricated on one Si die (14). Some of the possible modifications to enhance discrimination among molecules include transition metal overcoatings (13), alloys of Pd with Ag, Au, and other metals (14), and hot, noble metal wires in close proximity to facilitate dissociation of molecules that are normally inert on Pd to more reactive fragments (15). Although some insight into the choices of modifications can be gleaned from the catalysis literature (16) and from a basic understanding of surface chemistry on catalysts, there is ample room to advance the level of understanding of the physicochemical interactions between detectable molecules and catalytic gate, thin film devices.

The first Si field-effect chemical sensors were not based on catalytic gates; they were sensors for measuring pH and other ionic species in aqueous solution (often called ISFETs for ion-sensitive field-effect transistors) (17). The device physics behind the sensor response is the same as described above, but the origin of the concentration-dependent electrostatic field is more complicated than that above because it involves chemical equilibria on the dielectric surface (1). SiO_2 is inadequate for contact with the aqueous solution because of instabilities, so much recent research has involved coatings that are more durable, such as silicon nitride and even Langmuir-Blodgett membranes (18). Progress in this area was recently reviewed by Bergveld (19).

Recently, the sensitivity of field-effect-based sensors has reached new heights through the addition of a stage of chemical amplification, obtained by immunoassay techniques. An example of this amplification is the detection of urease: each urease molecule at the surface of an ISFET produces thousands of ammonia molecules per second when excess urea is introduced, the result being a pH change that is detected and further amplified by the field-effect device.

In a recent demonstration of such detection, a pH-sensitive light-addressable potentiometric sensor (LAPS), a close relative to the ISFET, was used by Bousse *et al.* to detect 4×10^7 urease

molecules immobilized on a small area of porous membrane (20). This demonstration builds on the technology developed a few years earlier by Janata (1) for incorporating enzymes into a thin polymer film on the surface of an ISFET. A very sensitive but more complex assay, capable of measuring 2 pg of single-stranded DNA, was also described (20). A "DNA sandwich" was formed after the arrangement linker-AB_{DNA}/DNA/AB_{DNA}-(urease)_n, where AB_{DNA} denotes an antibody to DNA, "-" denotes a covalent bond, and "/" denotes an antibody-antigen bond. The value of *n* in this case was such that one urease was bound for every 20 DNA bases along a strand. After incubation, the sandwich was immobilized on a porous membrane via the "linker" (biotin or streptavidin). The membrane was then placed in contact with the LAPS and urea was introduced to determine the amount of DNA present from the pH change. Although multiple steps are needed away from the device surface, this is a remarkable step toward the ultrasensitivity and sensitivity of the biochemical microsensor.

Acoustic Wave Sensors

A second physical transduction technique involves the use of acoustic waves to detect the accumulation of species in or on a chemically sensitive film. The technique originated with the use of quartz resonators, which were excited into thickness-shear resonance to monitor vacuum deposition of metals (21). The device is operated in an oscillator configuration, with changes in resonant frequency related to the areal mass density accumulated on the crystal face. These devices have been coated with chemically sensitive films to produce gas and vapor detectors (22) and have been operated in solution as liquid-phase microbalances (23).

Another class of acoustic wave sensors uses surface acoustic waves (SAWs) to probe the accumulation of species in a surface film. These devices use interdigital electrodes that are photolithographically formed on the surface of a piezoelectric crystal to excite and detect the surface wave (Fig. 3). The stress-free boundary condition imposed by the surface results in a mode of propagation that is confined to the surface and has acoustic energy distributed within one wavelength of the surface. This surface confinement of acoustic energy makes the SAW extremely sensitive to the properties of a surface film, particularly changes in its mass. The surface wave has two components of displacement, one normal to the surface and one in the direction of wave propagation. The translation of surface mass by these SAW displacement components leads to a change in surface wave velocity. Wenzel and White have shown that mass sensitivity can be further enhanced by propagating a wave in a very thin membrane (24).

The acoustic wave gravimetric technique can be extended to liquid-phase sensing in one of two ways. Because the SAW displacement component normal to the surface generates compressional waves in a contacting liquid, excessive attenuation of the SAW occurs that renders it unsuitable for liquid-phase measurements. A mode with exclusively in-plane surface displacement, such as the shear-horizontal acoustic plate mode, can, however, be used successfully (25): shear waves propagate poorly in liquids, so attenuation is minor. The quartz thickness-shear resonators described above also have no displacement normal to the surface, and thus, they function in contact with liquids. A second alternative is to use an acoustic mode with velocity slower than that of sound in the contacting liquid, such as the Lamb wave described in detail by Wenzel and White (24).

SAW sensors are typically operated in a two-port oscillator configuration: the signal from the output transducer is amplified and fed back to the input transducer. Changes in wave velocity caused by

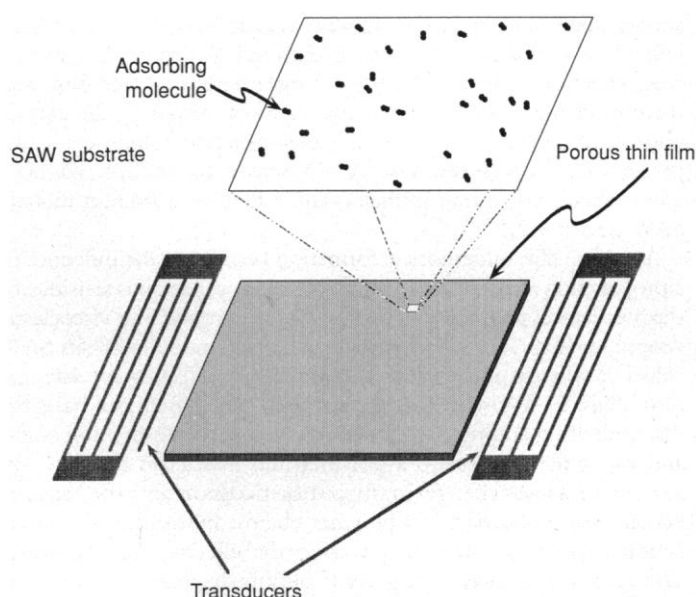


Fig. 3. A schematic of a SAW chemical sensor. The SAW substrate could be any piezoelectric material; quartz is often used. The size of the fingers composing the transducers is exaggerated; for high-frequency operation they must be only a few micrometers wide and a few micrometers apart.

species accumulation in a sorptive surface film cause proportional changes in oscillation frequency. The mass sensitivity of the SAW propagation velocity can be expressed as

$$\frac{\Delta v}{v_0} = -c_m f_0 \rho_s \quad (1)$$

where Δv is the change in the initial velocity, v_0 , $c_m = 1.29 \times 10^{-6} \text{ cm}^2 \text{ s g}^{-1}$ for SAWs propagating on ST-cut quartz (26), f_0 is the operating frequency, and ρ_s is the mass per unit area accumulated on the surface. At an operating frequency of 100 MHz and a frequency resolution of 1 Hz (limited by oscillator stability and the counting interval), the limit of mass resolution is 80 pg cm^{-2} ; this is equivalent to 0.3% of a monomolecular layer of N_2 .

A number of gas and vapor sensors have been realized by placing chemically sensitive films on SAW devices and relying on their extreme mass sensitivity. The first such sensor, reported by Wohltjen and Dessy in 1979 (27), detected a range of organic vapors by utilizing thin films of vacuum grease, oils, and waxes commonly used in gas chromatography. More than 100 papers have been published in this field since then, including several reviews (28, 29). Some of the most intensely studied areas include the following: (i) the use of organic polymer films to detect organic solvent vapors (30–33); (ii) the monitoring of small inorganic molecules, such as the halogens and the nitrogen and sulfur oxides, with organometallic films (for example, metal phthalocyanines) (34, 35) or metal oxides (36); (iii) humidity sensors based on organic polymer films (37, 38); and (iv) the detection of organophosphonates (simulants for and decomposition products of chemical warfare agents) (39, 40) with a variety of different thin film materials. Styrene has been detected by its reversible reaction with an organoplatinum compound (41).

Surface waves interact with film overlays in a number of ways, so that SAW propagation is influenced by factors other than mass density. Because the wave propagates in a piezoelectric medium, mechanical deformation of the substrate is accompanied by a propagating electric field. The acousto-electric interaction that occurs between this electric field and any charge carriers present in a

surface film results in changes in wave velocity and attenuation. This effect has been used as a basis for chemical detection: species that react chemically (that is, transfer charge) with a surface film, and thereby change film conductivity, cause a response. In certain regimes of film conductivity, this acoustic-electric response is much greater than the mass response. A NO_2 sensor, for example, has been constructed with a lead phthalocyanine film on a lithium niobate SAW device (42).

A surface film undergoes deformation because of the influence of a propagating SAW. Consequently, wave propagation is sensitive to the mechanical properties of the film and can probe film viscoelastic properties (43). The elastic component of film modulus affects SAW velocity, whereas inelastic (viscous) behavior affects wave attenuation. This SAW-viscoelastic interaction can be used as a basis for discriminating among chemical species (43). The absorption of gas and vapor molecules into a polymer film plasticizes the film and also causes a mass change. Plasticization occurs as absorbed species become dispersed between polymer chains, lubricating the interaction between chains and lowering the effective film viscosity. The incremental plasticizing contribution depends on molecular volume, whereas the mass response depends on molecular mass. The velocity response is typically dominated by mass loading, whereas attenuation depends only on the plasticizing effect; measurement of these two parameters thus provides information about both the size and molecular mass of the absorbed species. These parameters are often sufficient to differentiate among several organic vapors.

Figure 4 is a parametric representation of the dual responses measured as a polysiloxane film is exposed to several volatile organic compounds over a continuous range of partial pressures from zero to about 20% of the saturated vapor pressures at 20°C (44). The distinct locus of velocity and attenuation points generated by each vapor demonstrates the discrimination capability of this technique. At a given value of attenuation, the magnitude of the frequency shift is proportional to the liquid density of the absorbed vapor, whereas attenuation is proportional to species volume. This dual response forms the basis for simultaneously determining both the identity and concentration of a single chemical species.

Microsensors Based on Optical Fibers

Optical fibers offer a number of advantages for chemical sensing (45). This technology offers long-distance telemetry, freedom from electromagnetic interference, and small size (approximately that of a human hair). Furthermore, the basic components necessary for sensor applications are being developed by the optical communications industry. Optical communications systems and optical sensors have the same functional design. Both need a light source, a detector, and a method of transmitting the light from the source to the detector (the optical fiber). For optical communications, a modulator is used to impose the information to be transmitted on the light beam. For optical sensing, the sensing element replaces the modulator and again imposes information on the light beam. The similarity between these two functions means that the components, developed at great cost for optical communications, can effectively be used for optical sensing applications.

The sensing element can modify either the intensity, phase, or polarization state of the light, and physical sensors have been made that make use of all three techniques (46, 47). For chemical sensing, most transduction mechanisms have focused on intensity modulation (we include spectroscopy and fluorescence-based sensors in this group), with a small effort (48) aimed at utilizing phase-modulating sensors (interferometers) (49).

A major difference between optical communications and optical sensing is the nature of the signal. Optical communications signals are invariably digital, whereas optical fiber chemical sensor signals are invariably analog. Thus, a referencing method is necessary for sensor applications to correct for changes in the optical signal induced along the optical path by unwanted environmental effects, for example, temperature variations. The normal method of solving this problem is to use two different wavelengths of light, with the sensing element having a large effect on the light at one wavelength compared to the other. By taking a ratio of the two signals, one removes the unwanted environmental effects.

One approach to the development of new chemical sensors is to try to adapt conventional analytical chemistry techniques to optical fiber chemical sensing. Within this philosophy the most common chemical transduction mechanism that has been used is the fluorescence of an indicator molecule. The intensity or lifetime of the fluorescence depends on the presence or absence of the chemical species of interest. Here a conventional analytical chemistry technique (50) is adapted to chemical sensing by using optical fibers to deliver the exciting light and collect the fluorescence. This approach takes advantage of a large body of knowledge that already exists about molecular fluorescence. In the same vein, dyes have been used that change absorbance with exposure to the chemical species to be detected (51). The dye is located at the end of optical fibers, and changes in either transmission or reflection of light are used to monitor the presence of the chemical species to be detected. Again, advantage is taken of an established analytical technique (52).

Similarly, optical fiber chemical sensors have been demonstrated that utilize Raman spectroscopy and absorption spectroscopy. However, simple vibrational spectroscopy techniques are not as easily extended to optical fiber chemical sensing because most optical fibers are not transparent in the infrared region of the spectrum, where most of the fundamental absorption bands exist. The development of new optical fiber materials (53) and integrated optical devices that can operate in this region of the spectrum should eventually lead to the ultimate optical fiber chemical sensor, one that has good sensitivity and great selectivity and can detect and identify thousands of compounds in complex measurement environments.

Some new chemical transduction mechanisms (not previously used for chemical analysis) are being explored that offer very high

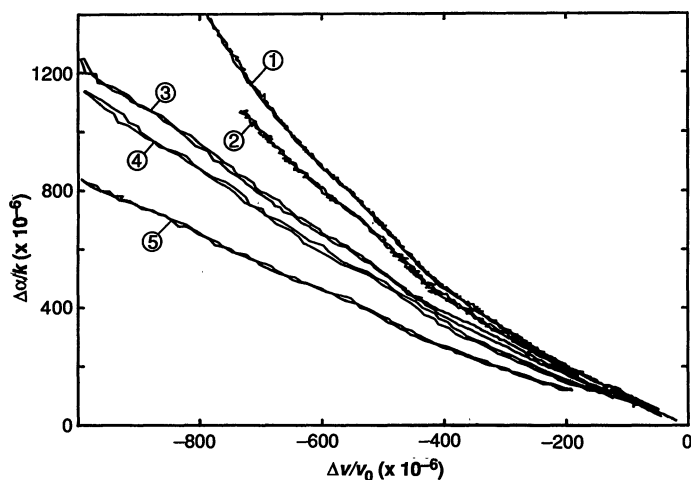


Fig. 4. Data obtained when a polysiloxane film is the "porous thin film" of Fig. 3. This is a plot of attenuation response ($\Delta\alpha/k$) versus frequency response ($\Delta\nu/\nu_0$) (1, hexane; 2, toluene; 3, methanol; 4, trichloroethylene; 5, dibromomethane). The curve for each molecule is unique, so molecular discrimination is possible. Each curve is generated by a ramp of the partial pressure starting at the right-hand side, followed by decreasing pressure, showing reversibility. The actual maximum vapor pressures shown are less than about 20% of the saturation partial pressure at 20°C for each vapor (for example, 9 torr for trichloroethylene).

sensitivity in limited measurement environments. One is the micromirror chemical sensor that uses changes in the reflectivity of thin coatings on the end of an optical fiber (54). Using semitransparent metal films (~ 100 Å thick), one can observe changes in reflectivity from the chemisorption of submonolayer coverages of molecules on the metal surface. These changes reflect the nature of the chemisorption bond as well as the optical properties of the chemisorbed atom or molecule. With a fiber core ($50\text{ }\mu\text{m}$ in diameter) defining the size of the sensing area, the presence of less than 10^8 mercury atoms has been detected with thin gold films (55). Similarly, the presence of less than one billion trichloroethylene (TCE) molecules has been detected with a thin polymer coating on the end of the fiber (56). For this sensor a plasma-polymerized tetrafluoroethylene film is deposited on the end of the fiber, forming a small optical cavity. The polymer absorbs the TCE and swells. The change in dimensions of the optical cavity changes its reflectivity. By using smaller core fibers and optimizing signal-to-noise ratios, one should be able to detect the presence of less than one million atoms or molecules with this technique.

Research on optical fiber-based chemical sensors is a very active area. The recent availability of the necessary components and the primary emphasis of past research on physical sensing applications mean that these techniques have been slow developing with respect to other chemical sensing techniques. No optical fiber chemical sensors are presently commercially available. Some are likely to come on the market in the near future, and optical fiber chemical sensors should have a large impact in the environmental monitoring and process control fields.

Electrochemical Microsensors

The most successful chemical microsensor in wide use today is the oxygen₂ sensor found in the exhaust system of almost all modern automobiles. It is an electrochemical sensor that uses a solid electrolyte, often doped ZrO_2 , as an oxygen ion conductor. The sensor is usually a small cup of the ceramic, with the reference side exposed to ambient air and the inside exposed to the exhaust. Both sides have catalytic (Pt) electrodes to facilitate equilibrium between O_2 and the oxygen ion in the ceramic, and the voltage output of the cell indicates the oxygen partial pressure in the exhaust; it is basically an electrochemical concentration cell. This sensor underwent many years of intense development, largely by the automobile companies; Logothetis has reviewed much of the work (57). The sensor illustrates many of the properties desired by other users for chemical microsensors: it works in a process control situation with very fast response time (~ 100 ms) for feedback control; it is relatively inexpensive because it is designed specifically for the one task and is mass-produced; and it performs in a very hostile environment and is reliable over a long period of time.

Nevertheless, there are shortcomings that are being addressed in current research. The sensor must be very hot ($>400^\circ\text{C}$) to give proper readings. Current models use a built-in heater so engines function properly when first started. The sensor works best at a near-stoichiometric fuel-air mixture; in rich mixtures, the available O_2 is burned completely on the Pt electrode and it is difficult to estimate the actual O_2 concentration. Recent attempts to solve this problem and lower the operating temperature include the use of thin films of SrTiO_3 (58) and a clever oxygen pump that combines two ZrO_2 membranes, one to read the O_2 partial pressure as described above and a second to supply electrochemically pumped O_2 to titrate excess fuel (59).

The success of the O_2 sensor has made the automobile manufacturers anxious to extend chemical sensing to a variety of tailpipe

gases: CO , NO_x , and short-chain hydrocarbons. Considerable research and development is needed for these molecules to be monitored in the hostile exhaust system environment.

Ion-selective electrodes and amperometric cells have had a long history of success in a wide variety of applications (1), although this success is not as dramatic in the daily lives of citizens as that of the O_2 sensors in automobiles. A microelectronics-inspired revolution is also occurring in these devices with the advent of photolithographically defined arrays of microelectrodes on planar substrates. Morita, Longmire, and Murray (60) have pointed out some of the advantages of these planar devices. One of the most important is that currents in relatively resistive media, even solid dielectrics, can be measured because the ratio of the electrode area to the space between electrodes ($1\text{ }\mu\text{m}$ or less) can be very large, resulting in lower resistance. The sample volumes are also very small, giving fast kinetics and gas-electrolyte equilibria as well as access to media too resistive for normal electrochemical cells. Some devices are so small that access to the volume of a living cell is possible. The low cost of manufacturing in quantity means that the devices can be disposable, thus avoiding some of the poisoning problems encountered with semipermanent macroscopic electrodes.

Coatings on the electrodes have yielded many provocative chemical-sensing structures (1, 60). A sensor that mimics the biological ion channel was reported (61); a Langmuir-Blodgett film coating was used that changed its permeability to redox ions in the presence of a "stimulus" species (such as Ca^{2+} ion).

Recent progress has been made in eliminating the need for a separate reference electrode (62), which reduces the complex three-electrode measurements to the simpler two-electrode configuration. The relatively new method of forming surface-attached monolayers by the self-assembly process was used with molecules that have pendant electroactive redox groups. Two redox species, one with an analyte-dependent electrochemical potential and the other with an analyte-insensitive electrochemical potential, are co-deposited on the working electrode with low surface area. The electrochemical potential difference between the two redox couples, measured by cyclic voltammetry, is an indication of the analyte concentration.

Another class of electrode coating that is attracting attention is the conducting organic polymers, typified by polypyrrole. For certain conducting polymers, microelectrode arrays allow monitoring of the film resistance over many decades without the need for a liquid phase. These films change conductivity in response to strongly oxidizing and reducing gases (63), which can "dope" the semiconducting polymer by adding or removing charge carriers, although the exact mechanism of conduction is still debated (64). Under certain conditions, less reactive species such as methanol also appear to affect the conductivity of these materials. Much of the data are empirical (65), and the understanding of the interactions leading to conveniently measured conductivity changes is not yet at the point at which sensing of a particular molecule can be predicted from the electronic structure of the organic polymer film.

Opportunities in Chemical Microsensors

Rapid progress in the design and understanding of chemical transduction mechanisms is occurring, but a tremendous amount of development work remains to bring the basic sensor into a functioning chemical detection system that works in the field. The environments in which these sensors must function are often very hostile to the life expectancy and operation of the sensor (Table 1). There may be wide temperature fluctuations (for example, a liquid hydrogen leak) in addition to other chemicals that interfere with the signal from the molecule of interest or permanently damage the

transducers. Yet, as Janata has pointed out (66), many papers often tell the reader little about how well and how long the sensor being discussed would perform in a variety of often hostile environments.

Materials science should play a leading role in the future of the interfacial chemical elements of microsensors. In this article we have discussed only a few of the advances that are already impacting sensors: sol-gel porous ceramics, plasma-polymerized films, Langmuir-Blodgett films with active groups incorporated, self-assembling monolayers, and conducting organic polymers. Much remains to be done with these materials and with virtually any other class of materials that changes one physical property or another as a result of interactions with chemical species in the ambient.

The biochemical sensor of the moth includes much more than just a sensing element. It has machinery to move the molecule from the gas phase into an aqueous phase, deliver it to the sensor, and later dispose of it to prevent saturation of the sensors. These "housekeeping" chores also have to be performed in one way or another with most chemical microsensors, and for most uses some form of periodic calibration is required as well. There is some very interesting work on automating and miniaturizing these tasks; Manz *et al.* have given a recent discussion (67). One of the most promising avenues is the use of the micromachining of silicon to provide valves, pumps, storage volumes, and so forth, all on one chip, which could be integrated with any of the physical transducers we have described. Although it is clear that no single sensor methodology can satisfy all of the needs for chemical information, the groundwork is being laid for a toolbox of sensors that can be applied to a wide variety of chemical-sensing problems.

REFERENCES AND NOTES

1. J. Janata, *Principles of Chemical Sensors* (Plenum, New York, 1989).
2. M. J. Madou and S. R. Morrison, *Chemical Sensing with Solid State Devices* (Academic Press, New York, 1989).
3. R. W. Murray *et al.*, Eds., *Chemical Sensors and Microinstrumentation*, no. 403 of the *ACS Symposium Series* (American Chemical Society, Washington, DC, 1989).
4. D. Schuetzle and R. Hammerle, Eds., *Fundamentals and Applications of Chemical Sensors*, no. 309 of the *ACS Symposium Series* (American Chemical Society, Washington, DC, 1986).
5. S. M. Sze, *Physics of Semiconductor Devices* (Wiley Interscience, New York, ed. 2, 1981), chap. 5.
6. D. Schneider, *Sci. Am.* **231**, 28 (July 1974).
7. E. A. Richard and C. Miller, *Science* **247**, 1208 (1990).
8. M. Barinaga, *ibid.* **250**, 506 (1990).
9. S. Oiki, W. Danho, M. Montal, *Proc. Natl. Acad. Sci. U.S.A.* **85**, 2393 (1988).
10. I. Lundström and D. Soderberg, *Sens. Actuators* **2**, 105 (1981).
11. R. C. Hughes and R. Bastasz, *J. Appl. Phys.* **64**, 6839 (1988).
12. R. C. Hughes, P. A. Taylor, A. J. Ricco, R. R. Rye, *J. Electrochem. Soc.* **136**, 2653 (1989).
13. I. Lundström, A. Spetz, F. Winquist, U. Ackelid, H. Sundgren, *Sens. Actuators* **B1**, 15 (1990).
14. R. C. Hughes, W. K. Schubert, T. E. Zipperian, J. L. Rodriguez, T. A. Plut, *J. Appl. Phys.* **62**, 1074 (1987).
15. W. Hornik, *Sens. Actuators* **B1**, 35 (1990).
16. E. G. Allison and G. C. Bond, *Catal. Rev.* **7**, 233 (1972).
17. P. Bergveld, *IEEE Trans. Biomed. Eng. BME-17*, 70 (1970).
18. A. Vogel, B. Hoffmann, S. Schwegel, G. Wegner, *Sens. Actuators* **B4**, 65 (1991).
19. P. Bergveld, *ibid.*, p. 125.
20. L. Bousse, G. Kirk, G. Sigal, *ibid.* **B1**, 555 (1990).
21. G. Z. Sauerbrey, *Z. Phys.* **155**, 206 (1959).
22. T. Nakamoto and T. Moriizumi, *Proceedings of the IEEE Ultrasonics Symposium*, 2 to 5 October 1988, Chicago, IL (IEEE, New York, 1988), pp. 613–616.
23. T. Numura and A. Minemura, *Nippon Kagaku Kaishi* **1980**, 1621 (1980).
24. S. W. Wenzel and R. M. White, *Sens. Actuators* **A21-23**, 700 (1990).
25. S. J. Martin, A. J. Ricco, T. M. Niemczyk, G. C. Frye, *ibid.* **20**, 253 (1989).
26. S. J. Martin, A. J. Ricco, D. S. Ginley, T. E. Zipperian, *IEEE Trans. Ultrason. Ferroelectr. Freq. Control* **UFFC-34**, 142 (1987).
27. H. Wohltjen and R. Dessy, *Anal. Chem.* **51**, 1465 (1979).
28. D. S. Ballantine, Jr., and H. Wohltjen, *ibid.* **61**, 704A (1989).
29. M. S. Nieuwenhuizen and A. Venema, *Sens. Mater.* **1**, 261 (1989).
30. H. Wohltjen, A. W. Snow, W. R. Barger, D. S. Ballantine, *IEEE Trans. Ultrason. Ferroelectr. Freq. Control* **UFFC-34**, 172 (1987).
31. J. W. Grate *et al.*, *Anal. Chem.* **60**, 869 (1988).
32. W. M. Heckl, F. M. Marassi, K. M. R. Kallury, D. C. Stone, M. Thompson, *ibid.* **62**, 32 (1990).
33. G. C. Frye and S. J. Martin, *Sens. Mater.* **2**, 187 (1991).
34. M. S. Nieuwenhuizen and A. J. Nederlof, *Anal. Chem.* **60**, 230 (1988).
35. A. W. Snow, W. R. Barger, M. Klusty, H. Wohltjen, *Langmuir* **2**, 513 (1986).
36. J. F. Vetelino, R. K. Lade, R. S. Falconer, *IEEE Trans. Ultrason. Ferroelectr. Freq. Control* **UFFC-34**, 156 (1987).
37. J. G. Brace, T. S. Sanfelippo, S. G. Joshi, *Sens. Actuators* **14**, 47 (1988).
38. S. J. Martin, G. C. Frye, A. J. Ricco, T. E. Zipperian, *Proceedings of the IEEE Ultrasonics Symposium*, 14 to 16 October 1987, Denver, CO (IEEE, New York, 1987), pp. 563–567.
39. J. Lint, H. Wohltjen, N. L. Jarvis, A. W. Snow, in *Fundamentals and Applications of Chemical Sensors*, no. 309 of the *ACS Symposium Series*, D. Schuetzle and R. Hammerle, Eds. (American Chemical Society, Washington, DC, 1986), p. 155.
40. J. W. Grate, A. Snow, D. S. Ballantine, H. Wohltjen, *Anal. Chem.* **60**, 864 (1988).
41. E. T. Zellers, N. Hassold, R. M. White, S. M. Rappaport, *ibid.* **62**, 1227 (1990).
42. A. J. Ricco, S. J. Martin, T. E. Zipperian, *Sens. Actuators* **8**, 319 (1985).
43. S. J. Martin and G. C. Frye, *Appl. Phys. Lett.* **57**, 1867 (1990).
44. G. C. Frye and S. J. Martin, *Proceedings of Transducers '91*, 24 to 27 June 1991, San Francisco, CA (IEEE, New York, 1991), pp. 566–569.
45. C. Yeh, *Handbook of Fiber Optics, Theory and Applications* (Academic Press, New York, 1990).
46. J. Dakin and B. Culshaw, *Principles and Components*, vol. 1 of *Optical Fiber Sensors* (Artech House, London, 1988).
47. J. Dakin and B. Culshaw, *Systems and Applications*, vol. 2 of *Optical Fiber Sensors* (Artech House, London, 1989).
48. R. A. Lieberman and M. T. Wlodarczyk, Eds., *Proceedings of Chemical, Biochemical, and Environmental Fiber Sensors II*, 19 to 21 September 1990, San Jose, CA (SPIE, Bellingham, WA, 1991).
49. The development of fiber optic chemical sensors has been slower than other chemical-sensing techniques, and, for this reason, not many general sources of information such as books and review articles exist. The best source of current research in the field is the proceedings of the chemical, biochemical, and environmental fiber sensors symposium held each year by the Society of Photo-Optical Instrumentation Engineers (SPIE) [see (48)].
50. I. M. Warner, in *Instrumental Analysis*, G. D. Christian and J. E. O'Reilly, Eds. (Allyn Bacon, Boston, 1986), chap. 9.
51. J. I. Peterson, S. R. Goldstein, R. V. Fitzgerald, D. K. Buckhold, *Anal. Chem.* **52**, 864 (1980).
52. K. L. Cheng and B. Y. Young, in *Instrumental Analysis*, G. D. Christian and J. E. O'Reilly, Eds. (Allyn Bacon, Boston, 1986), chap. 7.
53. S. J. Saggese, J. A. Harrington, G. H. Sigel, in (48), pp. 2–14.
54. M. A. Butler and A. J. Ricco, *Appl. Phys. Lett.* **53**, 1471 (1988).
55. ———, R. J. Baughman, *J. Appl. Phys.* **67**, 4320 (1990).
56. M. A. Butler, R. J. Buss, A. Galuska, *ibid.*, **70**, 2326 (1991).
57. E. M. Logothetis, in *Chemical Sensor Technology*, N. Yamazoe, Ed. (Elsevier, New York, 1991), vol. 3, p. 89.
58. J. Gerblinger and H. Meixner, *Sens. Actuators* **B4**, 99 (1991).
59. J. H. Visser, R. E. Soltis, L. Rimai, E. M. Logothetis, *Proceedings of Transducers '91*, 24 to 27 June 1991, San Francisco, CA (IEEE, New York, 1991), pp. 555–557.
60. M. Morita, M. L. Longmire, R. W. Murray, *Anal. Chem.* **60**, 2770 (1988).
61. M. Sugawara, K. Kojima, H. Sazawa, Y. Umezawa, *ibid.* **59**, 2642 (1987).
62. J. J. Hickman, D. Ofer, P. E. Laibinis, G. M. Whitesides, M. S. Wrighton, *Science* **252**, 688 (1991).
63. T. Hanawa, S. Kuwabata, H. Hashimoto, H. Yoneyama, *Synth. Met.* **30**, 173 (1989).
64. K. Sato, M. Yamaura, T. Hagiwara, K. Murata, M. Tokumoto, *ibid.* **40**, 35 (1991).
65. P. N. Bartlett and S. K. Ling-chung, *Sens. Actuators* **20**, 287 (1989).
66. J. Janata, *Anal. Chem.* **62**, 33 (1990).
67. A. Manz, N. Graber, H. M. Widmer, *Sens. Actuators* **B1**, 244 (1990).
68. This work was performed at Sandia National Laboratories and was supported by the U.S. Department of Energy under contract DE-AC04-76DP00789.